Evaluation of AMSR2 Thin Ice Area Extraction Algorithm Applied to the Sea Ice Zones of the Northern Hemisphere

Kohei Cho (1), Kazuhiro Naoki (1)

[1]Tokai University Research & Information Center (TRIC),
2-3-23, Takanawa, Minato-ku, Tokyo, 108-8619, Japan
Email: kohei.cho@tokai-u.jp, naoki@tokai-u.jp

Keywords: Sea ice, Passive microwave radiometer, GCOM-W, global warming

Abstract: Sea ice has an important role of reflecting the solar radiation back into space. In addition, the heat flux of ice in thin ice areas is strongly affected by the ice thickness difference. Therefore, ice thickness is important parameter of sea ice. For the past few years, the authors have been developing a thin ice area extraction algorithm using passive microwave radiometer AMSR2 for the Northern Hemisphere mainly focused in the Sea of Okhotsk. The basic idea of the algorithm is to use the brightness temperature scatter plots of AMSR2 19GHz polarization difference (V-H) vs 19GHz V polarization. The result was well evaluated by JAXA and was approved as the Research Product of AMSR2. The details of the algorithm and evaluation result applied to the sea ice zones of the Northern Hemisphere are presented in this paler.

1. INTRODUCTION

The earth observation with passive microwave radiometer started in 1978 by SMMR on board Nimbus-7. Since then, a series of passive microwave radiometers, including AMSR2 onboard GCOM-W satellite, have been continuously observing the earth for over 40 years. One of the main targets of the observation is sea ice. Since microwaves can penetrate clouds, the long-term sea ice extent could be derived from the passive microwave observation which showed clear decline trend of the Arctic sea ice cover (Comiso, 2012). The result was used as an evidence of global warming in the Fifth Assessment Report of IPCC (2014). The importance of sea ice monitoring from space using passive microwave radiometer is increasing. Usually, ice concentrations calculated from brightness temperatures measured by passive microwave radiometers are used for estimating the global sea ice extent. There are number of sea ice concentration algorithms including NASA Team Algorithm (Cavarieli et al., 1984) and Bootstrap Algorithm (Comiso, 1995). However, sea ice concentration only tells us the percentage of sea ice cover with in a footprint size of the radiometer. Ice thickness is another important parameter of sea ice. Studies on estimating ice thickness using passive microwave radiometers have been performed in the past including Tateyama et al. (2002), Martin et al. (2005), and Tamura et al. (2007). However, the detailed validation of the accuracy of the estimated sea ice thickness is still on the way. Our recent study suggested the limitation of estimating ice thickness from passive microwave radiometer observation (Naoki et al. 2018). The authors have developed a method to extract thin ice area using AMSR2 data (Cho et. Al, 2012, Tokutsu et. Al, 2014). The thin ice area extraction results were compared with simultaneously collected MODIS images for the Sea of Okhotsk for validation. It worked quite well in the Sea of Okhotsk. The algorithm was also applicable to the Bering Sea and the Gulf of St. Lawrence with some modification (Miyao et. Al., 2017, 2018, Cho et al., 2019). The algorithm has been approved by JAXA and the AMSR2 thin ice area data set using the algorithm will be released from JAXA in 2019 as one of the AMSR2 Research Products. This paper describes about the algorithm and the validation results performed in the sea ice zones of the Northern Hemisphere.

2. TEST SITES

In this study, three seasonal sea ice zones in the Northern Hemisphere namely the Okhotsk Sea, the Bering Sea, and the Gulf of St. Lawrence were selected as the test sites for the evaluation of thin ice area extraction. Figure 1 show the maps of the test sites. The Sea of Okhotsk and the Gulf of Se. Lawrence are seasonal sea ice zones. The Bering Sea is located at the northernmost part of the Pacific Ocean, surrounded by the Siberia, the Kamchatka Peninsula, the Alaska Peninsula and the Aleutian Islands. Basically, the sea is a seasonal sea ice zone. However, since it is connected to the Arctic Ocean by the Bering Strait, multi-year ice may come down through the strait. Moreover, it should be noted that the actual test site of the Bering Sea in this study included a part of the Arctic Ocean.

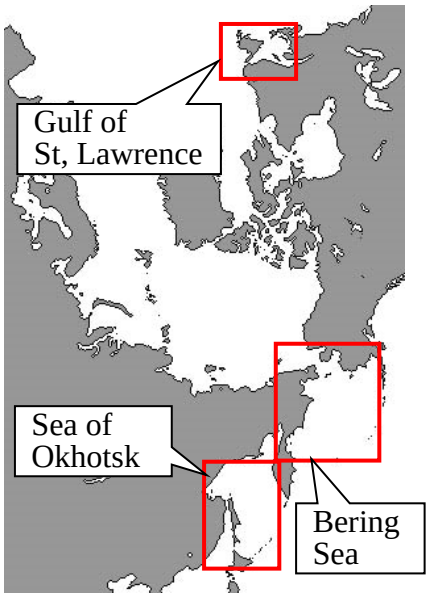

Figure 1. Map of the test sites (NSIDC, 2010)

3. ANALYZED DATA

The brightness temperature data acquired from passive microwave radiometer AMSR2 onboard GCOM-W satellite were used in this study. GCOM-W was launched by JAXA in 2012 and AMSR2 has been observing the earth for over 7 years. The diameter of the main reflector of AMSR2 is 2.0m, which is one of the largest reflectors used for passive microwave radiometer in space. Since the IFOV of a passive microwave radiometer depend upon the diameter size of the main reflector, the IFOV of each frequency of AMSR2 is one of the highest among similar sensors in space. Table 1 shows the specifications of AMSR2. The ice concentration data derived from AMSR2 data using Bootstrap Algorithm (Comiso, 2009) is also used in this study. In order to identify thin ice areas, data collected by optical sensor MODIS onboard Aqua satellite were used as reference. Table 2 show the specifications of MODIS. As for MODIS, only the Band 1 and 2 which have the highest IFOV of 250m among 36 bands were used in this study. Under the cloud free condition, detailed distribution of sea ice can be observed from MODIS images. Since Aqua and GCOM-W are in the same orbital "track" of the NASA's A-Train Program (NASA, 2010), the constellation of satellites, MODIS onboard Aqua observed the same area four minutes after the observation of AMSR2 onboard GCOM-W. Therefore, MODIS data is one of the most effective validation data for AMSR2 data.

Table 1. Specifications of AMSR2

Frequency (polarization)	IFOV	Swath	Incident angle
6.925GHz(V,H)	35×62 km	1450 km	55 deg
10.65GHz (V,H)	24×42 km		
18.7GHz(V,H)	14×22 km		
23.8GHz(V,H)	15×26 km		
36.5GHz(V,H)	7×12 km		
89.0GHz(V,H)	3×5 km		

Table 2. Specifications of MODIS

Band	Wavelength	IFOV	Swath
1	0.620-0.670 μm	250 m	2330 km
2	0.841-0.876 μm		

4. RESEARCH METHOD

4. 1. Sample area selection

Figure 2 show the comparison of simultaneously collected MODIS image and AMSR2 ice concentration (IC) image of the Sea of Okhotsk taken on February 27, 2013. The AMSR2 ice concentrations were derive from the AMSR2 data using AMSR Bootstrap Algorithm. The clear distribution of sea ice in the Sea of Okhotsk can be identified from the AMSR2 ice concentration image as shown on Figure 2(c). However, it is difficult to identify ice thickness differences or ice types from the image. Under the cloud free condition, detailed conditions of sea ice can be identified from the images taken by the optical sensor MODIS as sown on Figure 2(a). Through the comparison of the onsite sea ice thickness measurements with data collected by optical sensor on board satellites, the authors have verified that under the less snow cover and cloud free condition, thin sea ice areas, where the ice thicknesses are less than around 30cm, can be identified in MODIS images (Cho et. al., 2012). In this study, the color composite images of MODIS (Band 1 to blue and red, Band 2 to green) were used for selecting sample areas of thin sea ice, big ice floe, open water and mixed sea ice as shown on Figure2(b). In thick ice area, since the albedo of both Band 1 and 2 are high, the area appears in white in the MODIS color composite image. On the other hand, in thin ice area, the albedos of both bands are low, the area becomes dark. Especially, since the surface and around of thin ice are rather wet, the albedo of Band 2(near infrared) become much lower compared with that of Band 1(visible). As a result, most of the thin ice areas appear in dark purple in the MODIS color composite image as sown on Figure 2(a). In this study, the authors defined these dark purple sea ice areas in the MODIS images as thin ice areas.

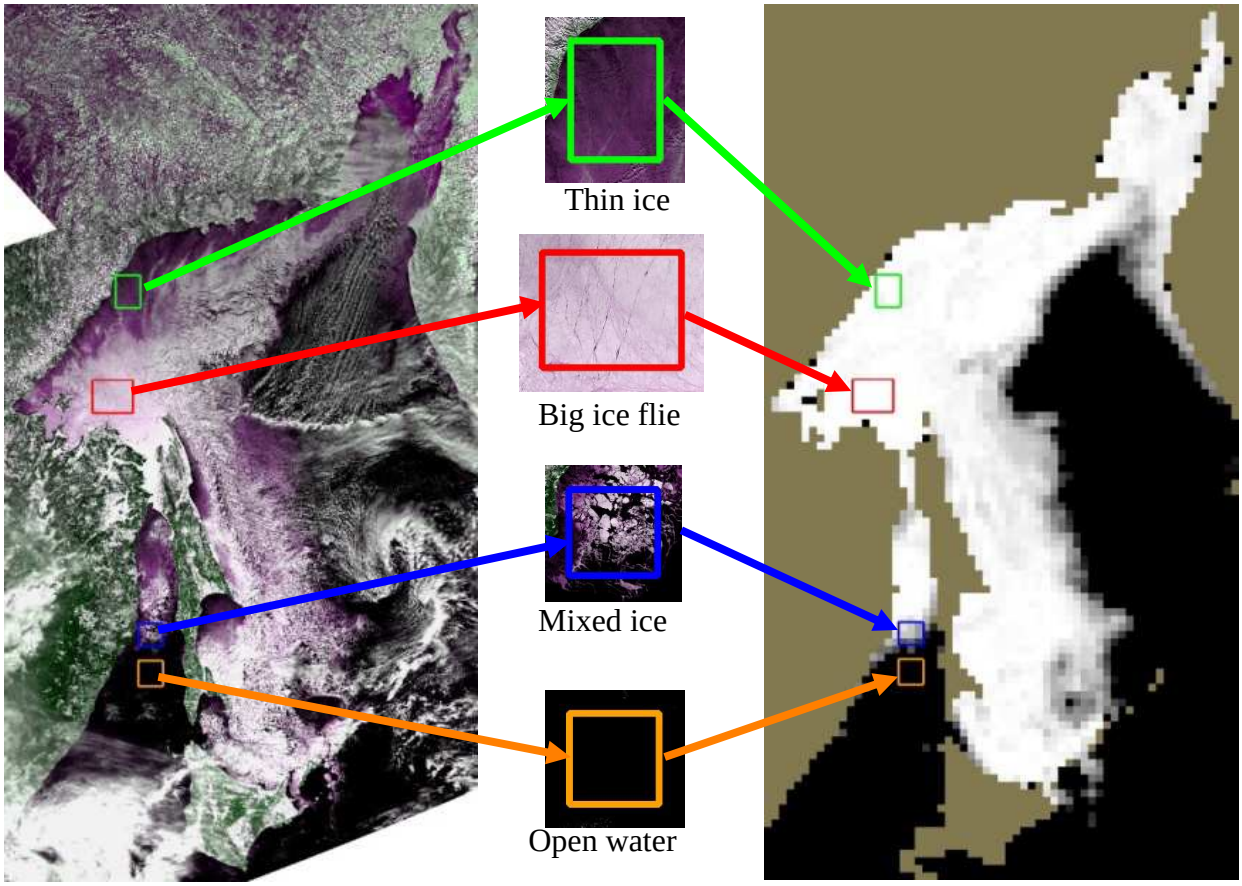

(a) MODIS image **(b) sample areas** **(C) AMSR2 IC image**

Figure2. Comparison of MODIS image and AMSR2 IC image.

(Sea of Okhotsk, February 27,2013)

4.2. Thin ice area extraction algorithm

The sample areas selected using MODIS image were overlaid on AMSR2 ice concentration image as shown on Figure 2. Then the AMSR2 brightness temperature of each sample area were plotted on the scattergram of AMSR2 19GHz V versus 19GHz (V-H) as shown on Figure 3. The brightness temperature of the sample areas extracted in Section 4.1 are plotted in different colors. ● represents open water, ✱ represents mixed ice, ▲ represents thin ice, and ■ represents big ice floe. In AMSR2 19GHz V polarization, the brightness temperature increases as the ice concentration increases. Since in low ice concentration sea ice area, sea ice and open water are mixed within one footprint size of a passive microwave radiometer, it is impossible to identify the difference of thin or thick. So, in this study, the thin ice areas are only extracted within high ice concentration areas. To do this, firstly we used the following equation to extract sea ice area with 80% or higher sea ice concentration.

$$(Tb19GHzV) > 245K \quad (1)$$

where Tb19GHzV: Brightness temperature of AMSR2 19GHz V polarization

The microwave brightness temperature of water is much lower in H polarization than in that of V polarization. As explained in Section 4.1, thin ice areas are rather wet. Therefore, in thin ice areas, the microwave brightness temperature of thin ice areas become much lower in H polarization than in that of V polarization. While the microwave brightness temperature of consolidated ice does not show big difference between V and H polarization. Considering these characteristics, the authors have introduced the following equation to differentiate thin ice area from consolidated ice.

$$(Tb19GHzV - Tb19GHzH) > -Tb19GHzV + 300K \quad (2)$$

where Tb19GHzH: Brightness temperature of AMSR2 19GHz H polarization

Since the brightness temperature difference between V and H polarization is much bigger for thin ice than for big ice floe, extraction of thin ice area can be expected using the equation (2). The parameters of the both equations were specified for the Sea of Okhotsk in our previous studies(Cho et. Al, 2012, Tokutsu et. Al, 2014). By using equation (1) and (2), the points distributed in yellow colored area will be classified as thin ice area.

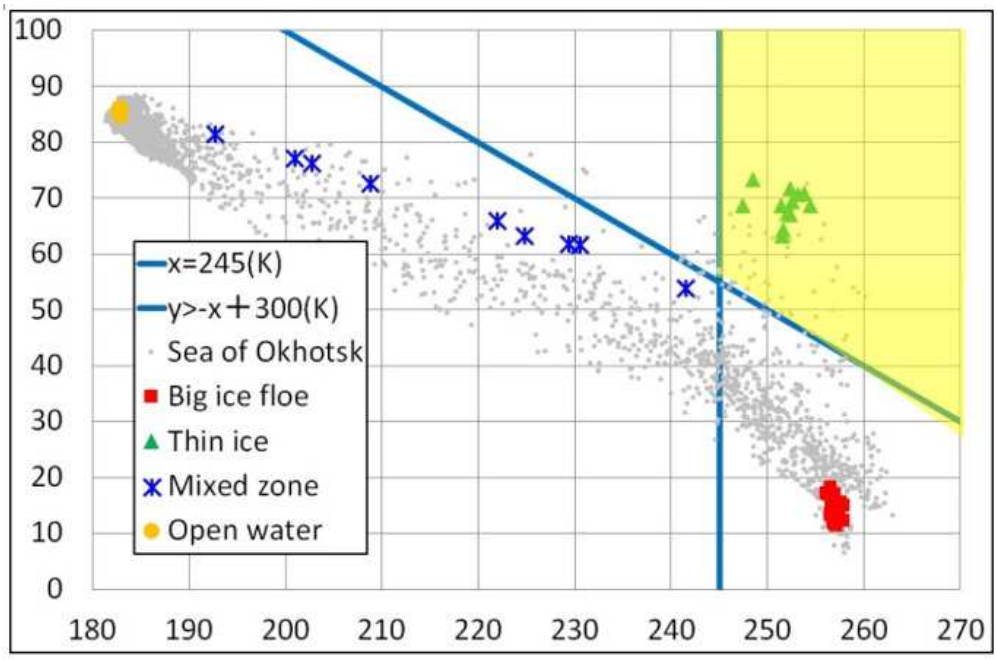

Figure 3. Scatter plots of (19GHzV – 19GHzH) Vs 19GHzVPolarization (Sea of Okhotsk, Feb. 27, 2013)

5. EXTRACTED RESULTS

5.1 Sea of Okhotsk

Firstly, the authors have applied the Thin Ice Algorithm to AMSR2 data of the Sea of Okhotsk. Figure 4(a) shows the AMSR2 sea ice concentration image of February 27, 2013. The cyan colored areas in the image show the "thin ice areas" extracted using AMSR2 data using equations (1) and (2). The extracted areas were overlaid on the simultaneously collected MODIS image for evaluation as shown on Figure 4 (b). It shows that not all but most of the thin ice areas which are appearing in dark purple in the MODIS image are extracted with the proposed method. The authors have applied the algorithm also to the AMSR2 data of the Sea of Okhotsk acquired on February 23, 2014 with good result (see Figure 5).

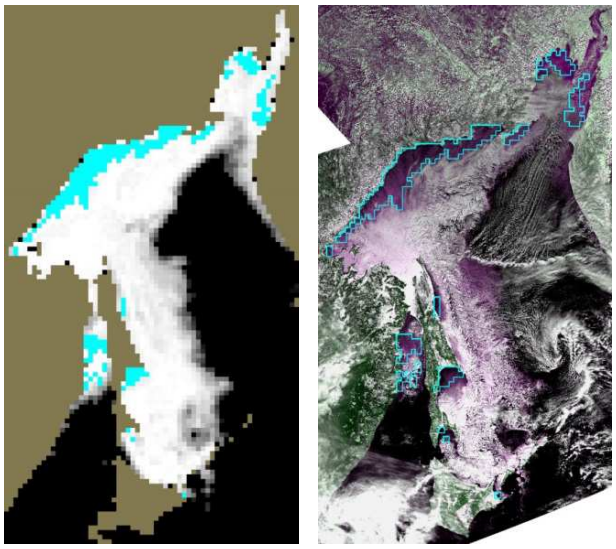

(a) AMSR2 IC image (b) MODIS image

Figure 4. Thin ice area extraction result (Sea of Okhotsk, Feb. 27, 2013)

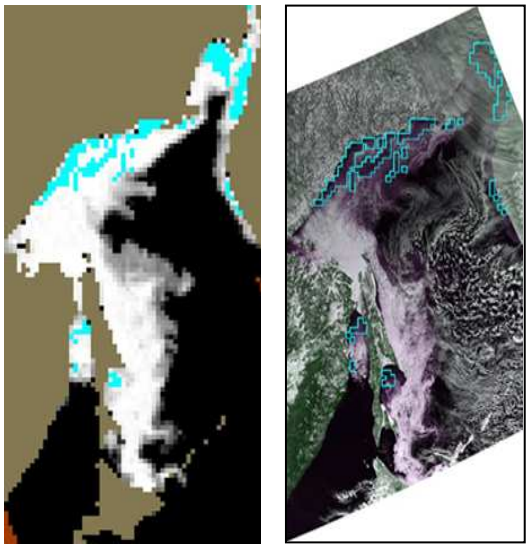

(a) AMSR2 IC image (b) MODIS image

Figure 5. Thin ice area extraction result (Sea of Okhotsk, Feb. 23, 2014)

5.2 Bering Sea

The same algorithm using equations (1) and (2) were applied also to t AMSR2 data of the Bering Sea taken on March 19, 2016. Figure 6 show the result. Most of the thin ice area recognized in the MODIS image were well extracted with AMSR2 data. However, a thin ice area which can be recognized in the MODIS image were not extracted with AMSR2 data (see the area indicated by the blue arrow in Figure 6).

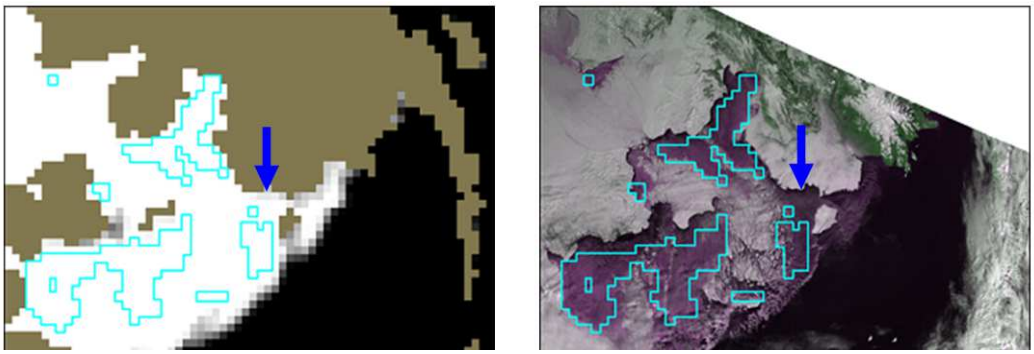

(a) AMSR2 IC image (b) MODIS image

Figure 6. Thin ice area extraction result. (Bering Sea, March 19, 2016)

So, the authors have selected sample areas of thin sea ice, big ice floe, open water, mixed sea ice and the unextracted thin ice area. Then the AMSR2 brightness temperature of each sample area were plotted on the scattergram of AMSR2 19GHz V versus 19GHz (V-H) as shown on Figure 7. The mark ■ shows the distribution of un-extracted thin ice area. This scatterplot suggested that the threshold of equation (1) need to be change from 245K to 235K for the Bering Sea. By applying this change to the algorithm, the un-extracted thin ice area were well extracted.

(Tb19GHzV)>235K (1)'

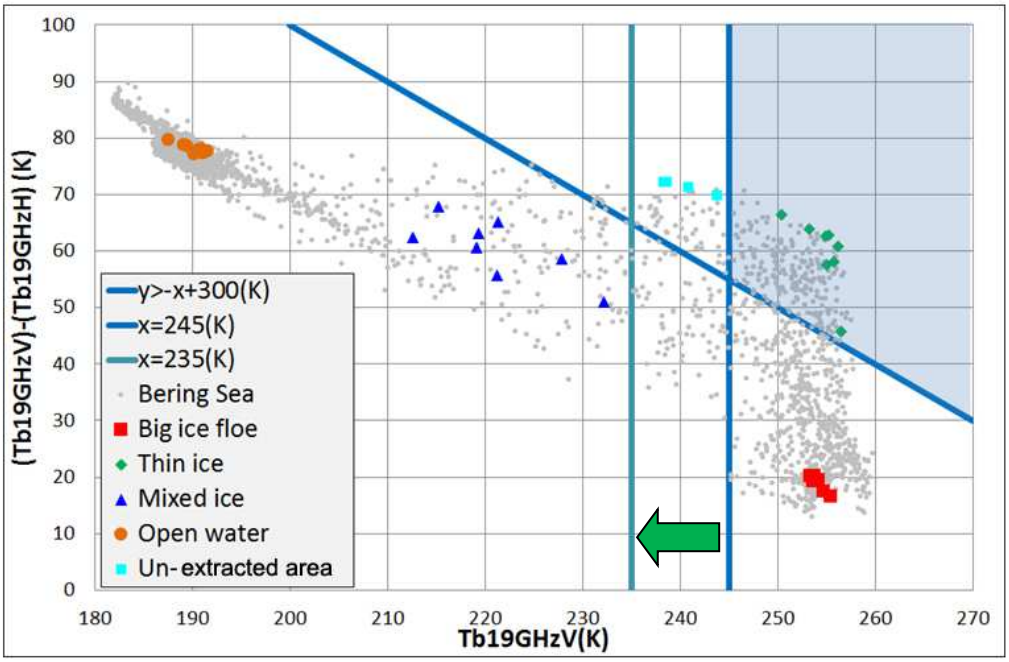

Figure 7. Scatter plots of (19GHzV – 19GHzH) Vs 19GHzV polarization (Bering Sea, March 19, 2016)

After the parameter tuning, the algorithm was also applied to the AMSR2 data of the Bering Sea acquired on February 10, 2014. The thin ice areas were well extracted. However, this time, some of the big ice floe area in the Arctic Ocean were mis-extracted as thin ice area (see the area indicated by the red arrow in Figure 8). So, the authors have selected sample areas of thin sea ice, big ice floe, open water, mixed sea ice and the mis-extracted thin ice area. Then the AMSR2 brightness temperature of each sample area were plotted on the scattergram of AMSR2 19GHz V versus 19GHz (V-H) as shown on Figure 9. It is clear that the mis-extracted points ● are distributed in the blue meshed area to be classified to thin ice area in the algorithm.

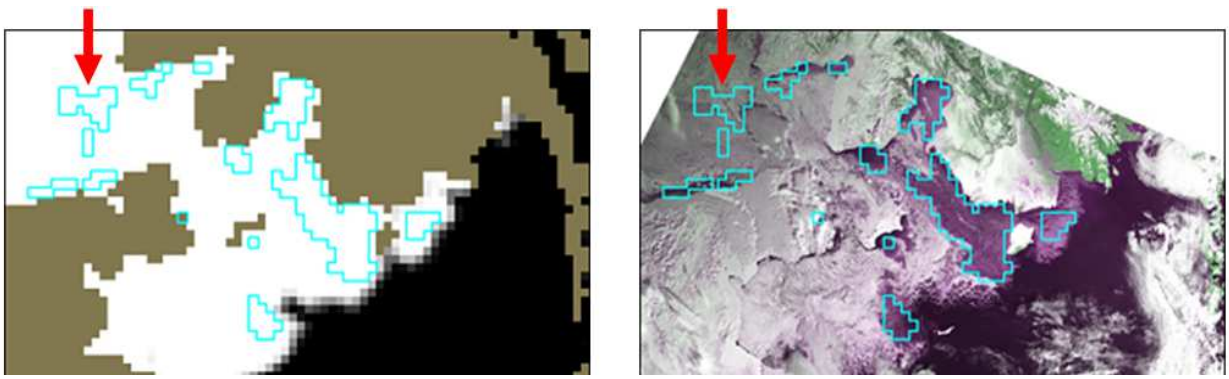

(a) AMSR2 IC image **(b) MODIS image**

Figure 8. Thin ice area extraction result (Cyan: extracted area) (Bering Sea, February 10, 2014)

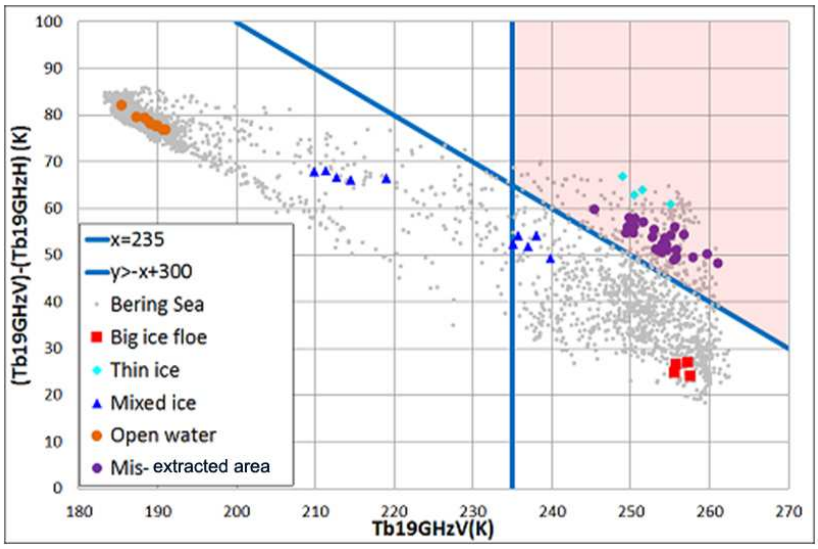

Figure 9. Scatter plots of (19GHzV – 19GHzH) Vs 19GHzV polarization (Bering Sea, February 10, 2014)

In order to solve the problem, the authors have re-examined the brightness temperature characteristics of mis-extracted thin ice, big ice floe, thin ice, mixed ice and open water as shown on Figure 10. Focusing attention on 19GHz, the polarization difference of the brightness temperature is large for thin ice than big ice floe. This is the reason we are using equation (2) for extracting thin ice area. However, the mis-extracted areas also show the brightness temperature similarly to the actual thin ice in both vertical and horizontal polarization. The water existence on and/or around the big ice floe may causing this phenomenon. On the other hand, if we focus on 89GHz, the brightness temperature difference between Vertical and Horizontal polarization in 89GHz is much larger in the thin ice area compared with that of the mis-extracted area. Considering these characteristics, the authors have decided to introduce the scattergram of AMSR2 19GHz V versus 89GHz (V-H) as shown on Figure 11. Considering this scatter plots, the authors have derived the equation (3) to reject the mis-extracted thin ice areas.

$$(Tb89GHzV - Tb89GHzH) > 20K \qquad (3)$$

where Tb89GHzV: Brightness temperature of AMSR2 89GHz V polarization
Tb89GHzH: Brightness temperature of AMSR2 89GHz H polarization

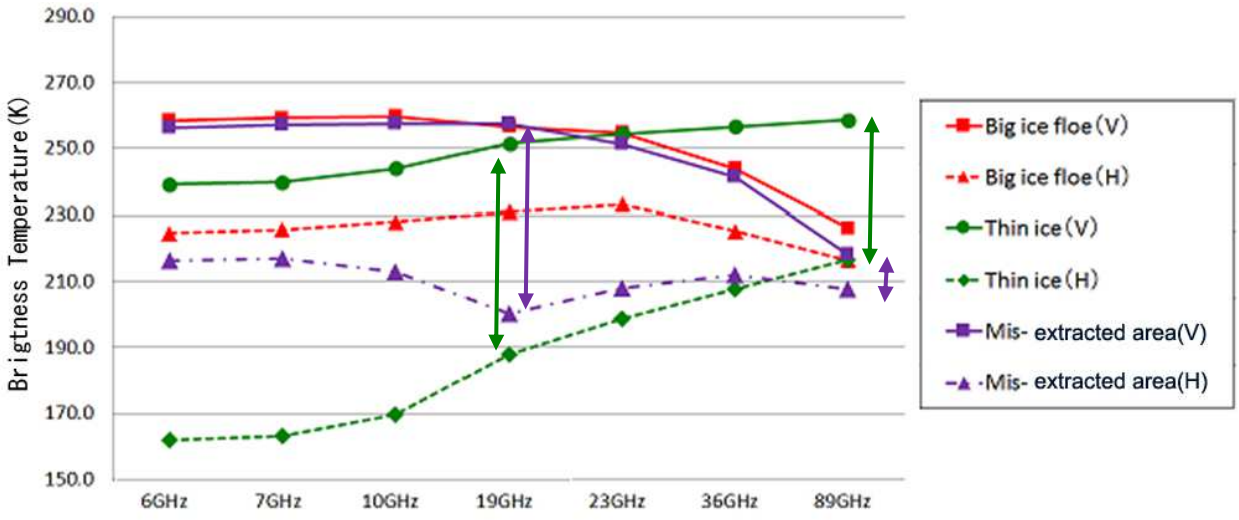

Figure 10. Brightness temperature characteristics graph of test area (Bering Sea, February 10, 2014)

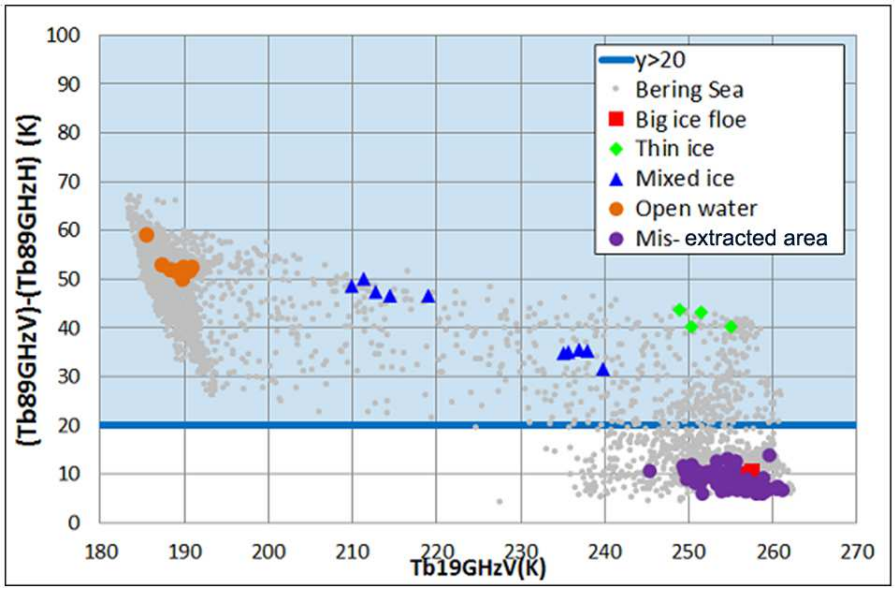

Figure 11. Brightness temperature characteristics graph of test area (Bering Sea, February 10, 2014)

Figure 12 show the result of applying equation (3) in addition to the original algorithm. The most of the mis-extracted thin ice areas over big ice floe as indicated by the red arrow in Figure 8 were well rejected without rejecting the other thin ice areas. The revised algorithm worked well also to the other scenes of the Bering Sea (Miyao et al., 2018).

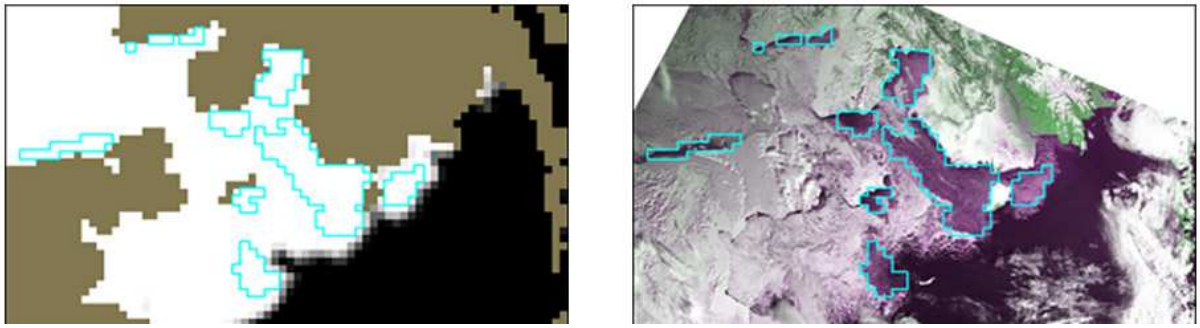

(a)AMSR2 IC image **(b) MODIS image**

Figure 12. Thin ice area extraction result. ((Bering Sea, February 10, 2014)

5.3 Gulf of St. Lawrence

The algorithm using equations(1)' and (2) was also applied to AMSR2 data of the Gulf of St. Lawrence acquired on March 1, 2015 as shown on Figure 13. Most of the thin ice area recognized in the MODIS image were well extracted.

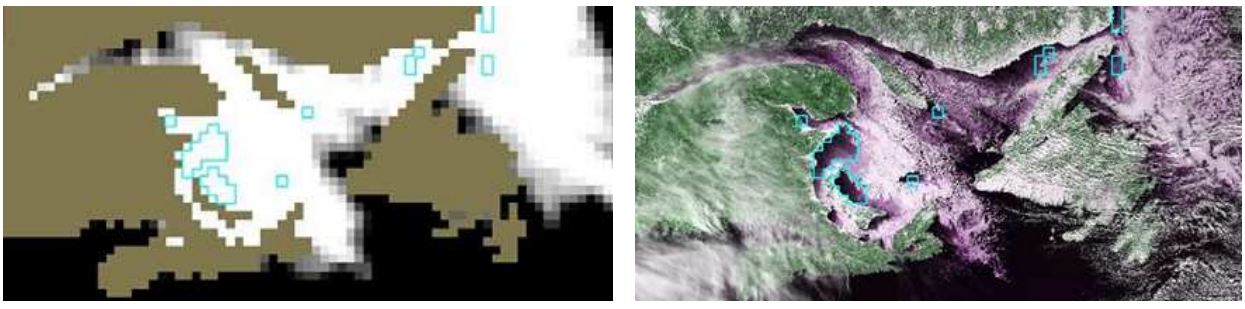

(a)AMSR2 IC image **(b) MODIS image**

Figure 13. Thin ice area extraction result. (Gulf of St. Lawrence, March 1, 2015)

6. CONCLUSIONS

In this study, authors have applied the AMSR2 thin ice area extraction algorithm (Cho et. Al, 2012) which was developed for the Sea of Okhotsk to the Bering Sea and the Gulf of St. Lawrence. The extracted thin sea ice areas were validated by comparing with simultaneously collected MODIS images. After analyzing several scenes of the Bering Sea, two problems became clear. One was some of the thin ice areas were not extracted, and the other was some of the big ice floe were mis-extracted as thin ice areas. To solve these problems, the authors have improved the thin ice area extraction algorithm by changing the threshold of previous equation and introducing a new equation using polarization difference between vertical and horizontal polarization of 89GHz. The algorithm validation was performed with ten scenes in the Sea of Okhotsk, five scenes in both the Bering Sea and the Gulf of St. Lawrence. The results suggested that the improved algorithm could work well at least in the above three seasonal sea ice zones of the Northern Hemisphere. Considering these results, JAXA has decided to release the AMSR2 thin ice area extraction data set of the Northern Hemisphere as the AMSR2 research product from 2019. The authors are planning perform to additional validations on adjusting parameters of the algorithm to different sea ice zones including those of the Southern Hemisphere.

ACKNOWLEDGEMENT

This study was supported by JAXA under the framework of GCOM-W Project. The authors would like to thank JAXA for their kind support. Also, the authors would like to thank the students of Tokai University namely Mr. Shu Sugiura, Kazuya Hayashi, Mr. Kenta Miyao, and Ms. Tomoko Kasuda who graduated after their great contribution to this study.

REFERENCES

Comiso, J., 2012, Large Decadal Decline of the Arctic Multiyear Ice Cover, Journal of Climate, Vol. 25, pp.1176-1193.

IPCC. 2014. "Summary for Policymakers." *In Climate Change 2013: The Physical Basis*. Contribution of Working Group I to the Fifth Assessment Report of the Intergovernmental Panel on Climate Change, edited by T.F. Stocker, D. Qin, G.K. Plattner, *et al*., Cambridge: Cambridge University Press.

Cavalieri, D. J. and P. Gloersen, 1984, Determination of sea ice parameters with the NIMBUS 7 SMMR, J. Geophys. Res., Vol.89, pp.5355-5369.

Comiso, J. C., 1995 ,SSM/I Sea Ice Concentrations Using the Bootstrap Algorithm", NASA Reference Publication 1380, Maryland, NASA Center for AeroSpace Information.

Tateyama K., H. Enomoto,, T. Toyota. and S. Uto, 2002, Sea ice thickness estimated from passive microwave radiometers, Polar Meteorol. Glaciol., National Institute of Polar Research, Vol. 16, pp.15-31.

Martin S. and R. Drucker, 2005, Improvements in the estimates of ice thickness and production in the Chukchi Sea polynyas derived from AMSR-E, GRL, Vol. 32, L05505

Tamura T., K. I. Ohshima, T. Markus, D. J. Cavalieri, S. Nihashi, N. Hirasawa, 2007, Estimation of Thin Ice Thickness and Detection of Fast Ice from SSM/I Data in the Antarctic Ocean, Journal of Atmospheric and Oceanic Technology, Vol. 24, pp.1757-1772.

Kazuhiro Naoki, Masashige Nakayama, Tomonori Tanikawa, Kohei Cho, 2018, The microwave brightness temperature observation of growing thin sea ice in tank experiment, AGU Fall Meeting, C31D-1567.

Cho, K., Y. Mochizuki, Y. Yoshida, 2012, Thin ice area extraction using AMSR-E data in the Sea of Okhotsk, Proceedings of the 33rd Asian Conference on Remote Sensing**,** TS-E6-3, pp.1-6.

Tokutsu Y., K. Cho, 2014, Thin Ice Area Extraction Algorithm Using AMSR2 Data for the Sea of Okhotsk, Proceedings of the 35th Asian Conference on Remote Sensing, OS-101, pp.1-6.
Miyao, K., T. Kasuda, K. Naoki, K. Cho, 2017, Thin Ice Area Extraction in the Bering Sea & the Gulf of St. Lawrence Using AMSR2 Data, Proceedings of the 38th Asian Conference on Remote Sensing, PS-04-ID-843, pp.1-4.
Miyao, K., K. Naoki, K. Cho, 2018, Upgrading thin ice area extraction algorithm using AMSR2 data, Proceedings of the 39th Asian Conference on Remote Sensing, Vol.5. pp.3163-3172.
Cho, K., K. Miyao, K. Naoki, 2019 Thin Ice Area Extraction in The Seasonal Sea Ice Zones of The Northern Hemisphere using ASMR2 Data, International Archives of the Photogrammetry Remote Sens. Spatial Information Sciences, XLII-3/W7, pp.5-9.
Comiso, J. C., 2009, Enhanced Sea Ice Concentrations and Ice Extent from AMSR-E Data, Journal of the Remote Sensing Society of Japan, Vol.29, No.1, pp.199-215.
Cho K., Y. Mochizuki, Y. Yoshida, H. Shimoda and C. F. CHEN, 2012, A study on extracting thin sea ice area from space, International Archives of the Photogrammetry, Remote Sensing and Spatial Information Sciences, Vol. XXXIX-B8, pp.561-566.
NASA, 2012, The Afternoon Constellation, https://atrain.nasa.gov/